

Chapter 23

Introduction to Term Structure Modeling

Contents

23.1	Introduction	353
23.2	The Binomial Interest Rate Tree	353
23.2.1	Term structure and its dynamics	356
23.2.2	An approximate calibration scheme	358
23.2.3	Calibrated binomial interest rate trees	359
23.3	Applications	362
23.3.1	Spread of non-benchmark option-free bonds	362
23.3.2	Interest rate futures	365
23.3.3	Fixed-income options	366
23.3.4	Dynamic immunization	367
23.3.5	Delta (hedge ratio)	368
23.3.6	Holding period return analysis	368
23.4	Volatility Term Structures	368

*How much of the structure of our theories
really tells us about things in nature,
and how much do we contribute ourselves?*
—Arthur Eddington (1882–1944) [760]

The high interest rate volatility, especially since October 6, 1979 [361], calls for stochastic interest rate models. Models are also needed in managing interest rate risks of securities with interest rate-sensitive cash flows. This chapter initiates the study of stochastic term structure modeling with the **binomial interest rate tree**. Simple as the model is, it illustrates most of the basic ideas underlying models to come. Its applications are also generic in that the pricing and hedging methodologies can be easily adapted to other models.

The idea is similar to the one used in option pricing. The current task, however, is complicated by the fact that the evolution of an entire term structure, not just a single stock price, is to be modeled. The multitude of interest rate models is also in sharp contrast to the single dominating model of Black and Scholes in option pricing.

23.1 Introduction

A stochastic interest rate model performs two tasks. First, it provides a stochastic process that defines future term structures. The ensuing dynamics must conform to economic rationality; for instance, the resulting interest rates and bond prices must not allow arbitrage profits. Second, the model should be “consistent” with the observed term structure [413]. This stochastic approach complements traditional term structure theories. The unbiased expectations theory, the liquidity preference theory, and the market segmentation theory can all be made consistent with the model by introducing assumptions about the stochastic process [576].

Modern interest rate modeling is often traced to 1977 when Vasicek [771] and Cox, Ingersoll, and Ross [205] developed simultaneously their influential models [157]. Merton’s earlier work in 1970 marked the starting point of the continuous-time methodology to term structure modeling [454, 582]. Early models were usually one-factor ones with the short rate being the single factor. Later on, researchers tried to deal with the undesirable features of one-factor models, chiefly the strong correlation between short and long rates, by incorporating more factors. These models all have fitting problems because the parameters have to be estimated, and the resulting process may not price today’s benchmark bonds correctly. An alternative approach pioneered by Ho and Lee in 1986 [414] took the market yield curve as given, making fitting almost a non-issue.

Recall that any riskless security having cash flow C_1, \dots, C_n should have a market price of

$$\sum_{i=1}^n C_i d(i), \quad (23.1)$$

where the market discount function $d(i)$ denotes the present value of one dollar at time i . This decomposition allows us to concentrate on zero-coupon bonds.

23.2 The Binomial Interest Rate Tree

The aim here is to construct an interest rate tree consistent with the observed term structure, specifically the yields and/or yield volatilities of zero-coupon bonds of all maturities. Models based on such a paradigm are usually called, somewhat misleadingly, **arbitrage-free** or **no-arbitrage models** [157, 413, 439]. This important idea is due to Ho and Lee. The alternatives are **equilibrium models** and Black-Scholes models.

The model is a binomial tree in which the logarithm of the future short rate obeys the binomial distribution. The limiting distribution of the short rate at any future time is hence lognormal. The idea of no-arbitrage models fitting the market term structure is parallel to that of implied volatility before. In both cases the market data are used to determine model parameters.

In the binomial interest rate process, a binomial tree of possible short rates for each future period is constructed. Every short rate is followed by two short rates for the following period. In Fig. 23.1, node A coincides with the start of period j during which the short

rate r is in effect. At the conclusion of period j , a new short rate goes into effect for period $j + 1$. This may take one of two possible values: r_l , the “low” short rate outcome at node B, or r_h , the “high” short rate outcome at node C. Each branch has a fifty percent chance of occurring in a risk-neutral economy [795].

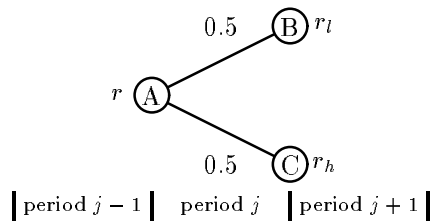


Figure 23.1: BINOMIAL INTEREST RATE PROCESS. From node A there are two equally likely scenarios for the short rate: r_l and r_h . Rate r is applicable to node A in period j . Rate r_l is applicable to node B and rate r_h is applicable to node C, both in period $j + 1$.

As the binomial process unfolds, we require that the paths combine. Suppose the short rate r can go to r_h and r_l with equal risk-neutral probability $1/2$ in a period of length Δt . The percent volatility of the short rate, $\Delta r/r$, is

$$\sigma = \frac{1}{2} \frac{1}{\sqrt{\Delta t}} \ln \left(\frac{r_h}{r_l} \right)$$

(see Exercise 23.2.2). In the above, σ is annualized, whereas r_l and r_h are period-based.

As

$$\frac{r_h}{r_l} = e^{2\sigma\sqrt{\Delta t}}, \quad (23.2)$$

greater volatility, hence uncertainty, leads to larger r_h/r_l and wider ranges of possible short rates. The ratio r_h/r_l changes across time if the volatility is a function of time. Note that r_h/r_l has nothing to do with r if σ is independent of r . To nail down the values of r_h and r_l , we need information from the current term structure to establish the relation between r and its two successors. Equation (23.2) will serve as the building block for the binomial interest rate tree.

We now proceed beyond the first period. In general, there are j possible rates in period j . According to the binomial process, the rates are

$$r_j, r_j v_j, r_j v_j^2, \dots, r_j v_j^{j-1},$$

where

$$v_j \equiv e^{2\sigma_j\sqrt{\Delta t}} \quad (23.3)$$

is the multiplicative ratio for the rates in period j (see Fig. 23.2). We shall call r_j the **baseline rate**. The subscript j in σ_j is meant to emphasize that the short rate volatility may be time-dependent.

One salient feature of the tree is path independence: The term structure at any node is independent of the path taken to reach it. Another nice property of the tree is that only the baseline rates (the r_i 's) and the multiplicative ratios (the v_i 's) need to be stored in computer memory in order to encode the whole tree. This takes up only $O(n)$ space. Throughout this chapter, n denotes the depth of the tree, i.e., the number of discrete time

periods. The naive approach of storing the whole tree would take up $O(n^2)$ space. This can be prohibitively expensive for a large tree. For instance, modeling daily interest rate movements for thirty years amounts to keeping an array of roughly $(30 \times 365)^2/2 \approx 6 \times 10^7$ double-precision floating-point numbers. If each number takes up eight bytes, the array would consume nearly half a gigabyte!

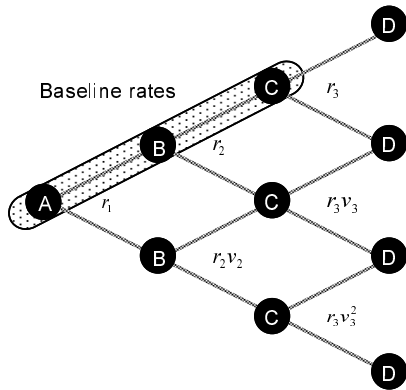


Figure 23.2: BINOMIAL INTEREST RATE TREE. The sequence at each time point shows that the short rate will converge to lognormal distribution.

Comment 23.2.1 An alternative process which also satisfies the path independence property is the following sequence of short rates for period j ,

$$r_j, r_j + v_j, r_j + 2v_j, \dots, r_j + (j - 1)v_j.$$

This is the original binomial interest rate model of Ho and Lee [414]. The model in this chapter, in contrast, is based on a model proposed by Black, Derman, and Toy [77]. If the j possible rates for period j are postulated to be $ru^{j-1}, ru^{j-2}d, \dots, rd^{j-1}$ for some common u and d , we have only u and d and possibly the transition probability to tune. With so few parameters, this model, due to Rendleman and Bartter [654], may not have enough degrees of freedom to fit the market term structure. \square

With the abstract process in place, concrete numbers are needed to set it in motion: They are the annualized rates of return associated with the various riskless bonds making up the benchmark yield curve and their volatilities. In the U.S., for example, the on-the-run yield curve obtained by the most recently issued Treasury securities may be used as the benchmark curve. The **term structure of (yield) volatilities** or simply the **volatility (term) structure** can be estimated from either historical data (historical volatility) or interest rate option prices such as cap prices (implied volatility) [132, 795]. The binomial tree should be consistent with both term structures. This chapter shall focus on the term structure of interest rates, deferring the handling of the volatility structure to §26.3.

In the limit, the short rate follows the following Ito process,

$$\frac{dr}{r} = \mu(t) dt + \sigma(t) dW,$$

or, equivalently,

$$d(\ln r) = \left(\mu(t) - \frac{1}{2} \sigma(t)^2 \right) dt + \sigma(t) dW,$$

where volatility $\sigma(t)$ is a deterministic function of time. The volatility (standard deviation) of the short rate one-period forward is approximately $r\sigma$ (see Exercise 23.2.2).

For economy of expression, all numbers in algorithms are measured by the period instead of being annualized whenever applicable and unless otherwise stated. Hence, before calling the algorithms, numbers should be converted to be period-based. The conversion is easy for volatility:

$$\sigma(\text{period}) = \sigma(\text{annual}) \times \sqrt{\Delta t}.$$

As for the interest rates, consult §3.1.

23.2.1 Term structure and its dynamics

Computing the **model price** from a binomial interest rate tree is easy thanks to its inductive nature: A security's value at a given node depends on its value at the two successor nodes. Refer back to Fig. 23.1. Given that the values at nodes B and C are P_B and P_C , respectively, the value at node A is simply

$$\frac{P_B + P_C}{2(1+r)} + \text{cash flow at node A}$$

by backward induction. To save computer memory, we compute the values column by column without explicitly expanding the binomial interest rate tree (see Fig. 23.3). Figure 23.4 contains the quadratic-time, linear-space algorithm. This algorithm is generic. It can be modified to handle any binomial short rate model: Just replace $r[i] \times v[i]^{j-1}$ in Step 2.1 with the short rate of the proposed model. Similarly, the methodology can be applied to trinomial trees.

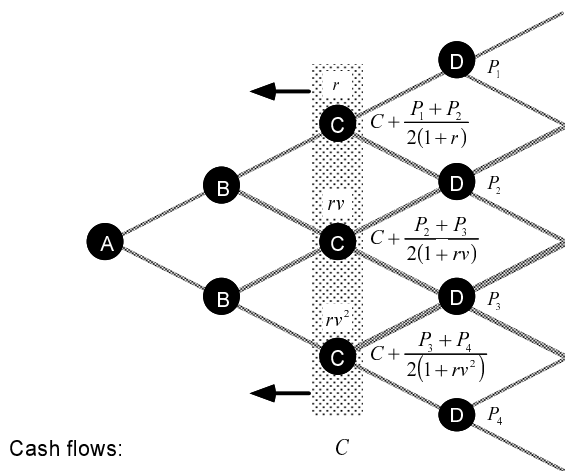


Figure 23.3: SWEEPING A LINE ACROSS TIME BACKWARD TO COMPUTE MODEL PRICE.

An n -period zero-coupon bond's price can be computed by assigning \$1 to every node at period n and then applying backward induction. Repeating this step for $n = 1, 2, \dots$, one obtains the market discount function implied by the tree. The tree therefore determines a term structure. It furthermore encompasses **term structure evolution** or **dynamics**, as taking any node in the tree as the current state induces a (smaller) binomial interest rate tree and, again, a term structure. The market discount function at node A in Fig. 23.2 evolves into another function at a B node and yet another function at a C node, and so on. The tree thus defines how the whole term structure moves through time.

Comment 23.2.2 Establishing the term structure dynamics of a binomial interest rate model can be costly. Suppose we want to know the m -period spot rate at time n , say, in order to price an instrument that matures then with a payoff linked to that spot rate. The tree has to be built all the way to time $n + m$ in order to obtain the price of the m -period zero-coupon bond at time n . This has dire performance implications. Later we will see cases where the tree only has to be built over the life of the derivative (n periods) instead of the life of the underlying asset ($n + m$ periods). \square

We shall construct interest rate trees consistent with the sample term structure in Fig. 23.5. This procedure is called **calibration**. For numerical demonstrations, volatility will be restricted to $v \equiv r_h/r_l = 1.5$, independent of time.

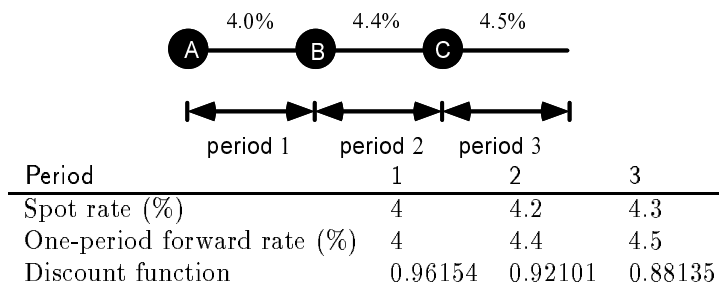


Figure 23.4: THE SAMPLE TERM STRUCTURE.

23.2.2 An approximate calibration scheme

This scheme starts with the implied one-period forward rates and their volatilities. For the first period, the forward rate is today's one-period spot rate. Proceed to the second period. Let the forward rate for the second period be f . Solve the following simultaneous equations,

$$\begin{aligned} r_h/r_l &= e^{2\sigma\sqrt{\Delta t}} \\ (r_h + r_l)/2 &= f \end{aligned} \quad (23.4)$$

The second equation states that the expected value of these two rates is identical to the forward rate. These equations have the following solutions,

$$r_h = \frac{2fe^{2\sigma\sqrt{\Delta t}}}{1 + e^{2\sigma\sqrt{\Delta t}}} \quad \text{and} \quad r_l = \frac{2f}{1 + e^{2\sigma\sqrt{\Delta t}}}. \quad (23.5)$$

Example 23.2.3 Suppose we are modeling the six-month short rate with a presumed annual percent volatility of 15%. Then $\Delta t \equiv 0.5$ and $r_h/r_l = \exp[2 \times 0.15 \times \sqrt{0.5}] = 1.2363$. If the forward rate for the same period is 8.00%, then

$$r_h = \frac{2 \times 0.08 \times 1.2363}{2.2363} = 0.08845 \quad \text{and} \quad r_l = \frac{2 \times 0.08}{2.2363} = 0.07155$$

by (23.5). \square

The principle embodied in (23.4) dictates that the expected short rate equal the forward rate. In other words, the unbiased expectations theory holds. In general, consider period j . Let f_j denote the forward rate for period j . Since the i th short rate, $1 \leq i \leq j$, occurs with probability $2^{-(j-1)} \binom{j-1}{i-1}$, this means $\sum_{i=1}^j 2^{-(j-1)} \binom{j-1}{i-1} r_j v_j^{i-1} = f_j$. So,

$$r_j = \left(\frac{2}{1 + v_j} \right)^{j-1} f_j. \quad (23.6)$$

The binomial interest rate tree is hence trivial to set up. Note that the forward rates f_j are related to the market discount function $d(i)$ via $f_j = (d(j)/d(j+1)) - 1$ by (5.7). The resulting tree for the sample term structure appears in Fig. 23.6.

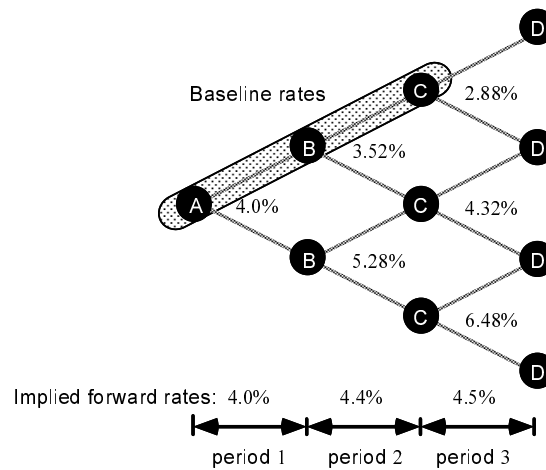


Figure 23.5: SAMPLE BINOMIAL INTEREST RATE TREE.

Let us carry out one numerical example with the tree in Fig. 23.6. The price of the zero-coupon bond paying \$1 at the end of the third period is

$$\begin{aligned} & \frac{1}{4} \times \frac{1}{1.04} \times \left(\frac{1}{1.0352} \times \left(\frac{1}{1.0288} + \frac{1}{1.0432} \right) + \frac{1}{1.0528} \times \left(\frac{1}{1.0432} + \frac{1}{1.0648} \right) \right) \\ &= 0.88155, \end{aligned} \quad (23.7)$$

which is very close to, but overestimates, the discount factor 0.88135. The tree, in a word, is not **calibrated**. That this approximation scheme overestimates the benchmark securities has been well documented [68, 795]. It can in fact be generalized as follows.

Theorem 23.2.4 The binomial interest rate tree constructed via (23.6) overestimates the prices of the benchmark securities as long as the volatilities are positive. This conclusion is independent of how, or whether, the volatility structure is fit. \square

23.2.3 Calibrated binomial interest rate trees

It is paramount for the binomial interest rate tree to generate model prices that match the observed market prices. This may well be the most crucial aspect of model building. To achieve it, we can treat the backward induction algorithm for the model price of the m -period zero-coupon bond in Fig. 23.4 as computing some function of r_m : $f(r_m)$. Now, apply

a good root-finding method to solve $f(r_m) = P$ for r_m given the m -period zero's market price P . Repeat this procedure for $m = 1, \dots, n$. The result is a cubic-time algorithm, which is hopelessly slow [163, 164, 462].

Calibration can be accomplished in quadratic time by **forward induction** [462]. The idea is to sweep a line across time *forward*. The algorithm inductively figures out how much \$1 at a node contributes to the model price. We shall call this number the **state price** since it stands for the price of a state contingent claim that pays \$1 at that particular node (state) and zero elsewhere.

Let us be more precise. Suppose we are at time j . So there are $j + 1$ nodes. Let the baseline rate for period j be $r \equiv r_j$, the multiplicative ratio be $v \equiv v_j$, and P_1, \dots, P_j be the state prices at the nodes of the previous period. By definition, $\sum_{i=1}^j P_i$ is the price of the $(j - 1)$ -period zero-coupon bond, or $d(j - 1)$. One dollar at time j has a known market value of $1/(1 + S(j))^j$, where $S(j)$ is the j -period spot rate. Alternatively, this dollar has a present value of

$$g(r) \equiv \frac{P_1}{(1+r)} + \frac{P_2}{(1+rv)} + \frac{P_3}{(1+rv^2)} + \dots + \frac{P_j}{(1+rv^{j-1})}.$$

So we solve

$$g(r) = \frac{1}{(1+S(j))^j} \quad (23.8)$$

for r . Given a decreasing market discount function, a unique positive solution for r is guaranteed because $g(r)$ is strictly decreasing with $g(0) = \sum_{i=1}^j P_i > 1/(1 + S(j))^j$ and $g(\infty) = 0$. The state prices for period j are then

$$\frac{P_1}{2(1+r)}, \frac{P_1}{2(1+r)} + \frac{P_2}{2(1+rv)}, \dots, \frac{P_{j-1}}{2(1+rv^{j-2})} + \frac{P_j}{2(1+rv^{j-1})}, \frac{P_j}{2(1+rv^{j-1})}$$

(see Fig. 23.7a). We call a tree with these state prices a **binomial state price tree**. Figure 23.7b depicts one such tree. As before, there is no need to explicitly store the whole tree of state prices.

Let us follow up with some numerical calculations. One dollar at the end of the second period should have a present value of 0.92101 according to the sample term structure. The baseline rate for the second period satisfies

$$\frac{0.480769}{1+r} + \frac{0.480769}{1+1.5 \times r} = 0.92101.$$

The result is $r = 3.526\%$. This is used to derive the next column of state prices shown in Fig. 23.7b as 0.232197, 0.460505, and 0.228308, whose sum gives the correct market discount factor: $0.232197 + 0.460505 + 0.228308 = 0.92101$. We proceed to solve for the baseline rate for the third period using

$$\frac{0.232197}{1+r} + \frac{0.460505}{1+1.5 \times r} + \frac{0.228308}{1+(1.5)^2 \times r} = 0.88135.$$

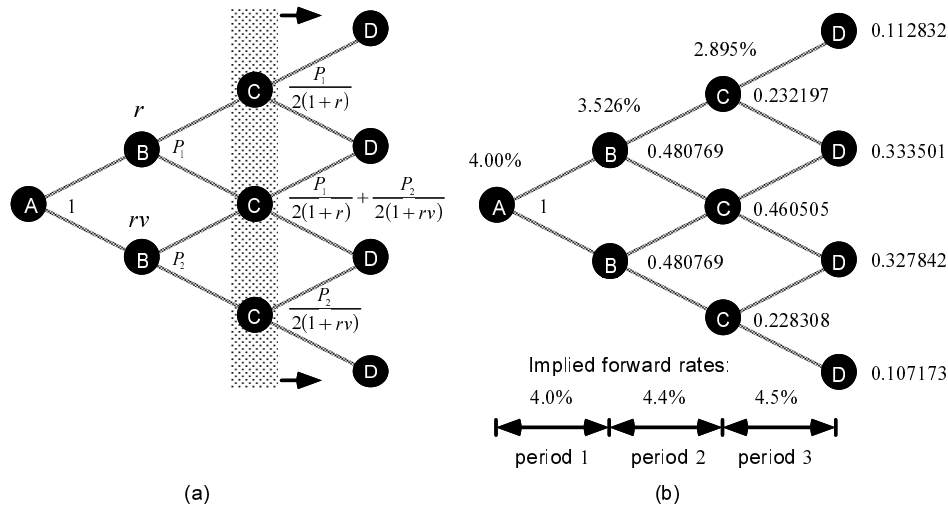


Figure 23.6: SWEEPING A LINE ACROSS TIME FORWARD TO COMPUTE BINOMIAL STATE PRICE TREE. (a) The state price at a node is a weighted sum of the state prices of its two predecessors. (b) The binomial state price tree calculated from the sample term structure and the resulting calibrated binomial interest rate tree. It prices the benchmark bonds correctly.

The result is $r = 2.895\%$. Now, redo (23.7), this time using the new ones,

$$\frac{1}{4} \times \frac{1}{1.04} \times \left(\frac{1}{1.03526} \times \left(\frac{1}{1.02895} + \frac{1}{1.04343} \right) + \frac{1}{1.05289} \times \left(\frac{1}{1.04343} + \frac{1}{1.06514} \right) \right) = 0.88135,$$

an exact match. The tree in Fig. 23.7b therefore prices without bias the benchmark securities giving rise to the sample term structure. The term structure dynamics of the calibrated tree is shown in Fig. 23.8.

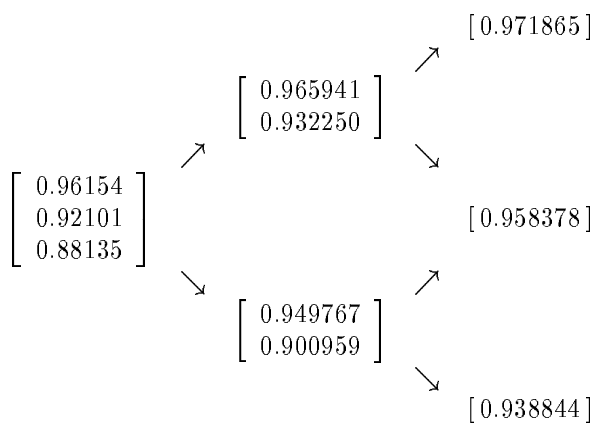


Figure 23.7: TERM STRUCTURE DYNAMICS. Each node lists the market discount function in increasing maturities.

The Newton-Raphson method can be used to solve for the r in (23.8) as $g'(r)$ is easy to evaluate. The monotonicity and convexity of $g(r)$ also facilitates root-finding. Finally, a good initial approximation to the root may be provided by (23.6), which is guaranteed to

underestimate the root (see Theorem 23.2.4). Using the previous baseline rate as the initial approximation to the current baseline rate also proves to be a successful strategy [550].

The above idea is straightforward to implement (see Fig. 23.9). The running time is $O(\mathcal{C}n^2)$, where \mathcal{C} is the maximum number of times the root-finding routine iterates, each consuming $O(n)$ work. With a good initial guess, the Newton-Raphson method converges in only a few steps [163, 164].

23.3 Applications

23.3.1 Spread of non-benchmark option-free bonds

Model prices calculated by the calibrated tree as a rule do not match market prices of non-benchmark bonds. To gauge the incremental return, or yield spread, over the benchmark bonds, we look for the spread uniformly over the short rates in the tree that makes the model price equal the market price.

It is best to illustrate the idea with an example. Start with the tree in Fig. 23.10. Consider a security with cash flow C_i at time i for $i = 1, 2, 3$. Its model price is

$$p(s) = \frac{1}{1.04 + s} \times \left[C_1 + \frac{1}{2} \times \frac{1}{1.03526 + s} \times \left(C_2 + \frac{1}{2} \left(\frac{C_3}{1.02895 + s} + \frac{C_3}{1.04343 + s} \right) \right) + \frac{1}{2} \times \frac{1}{1.05289 + s} \times \left(C_2 + \frac{1}{2} \left(\frac{C_3}{1.04343 + s} + \frac{C_3}{1.06514 + s} \right) \right) \right].$$

Given a market price of P , solving $P = p(s)$ for s gives us the spread.

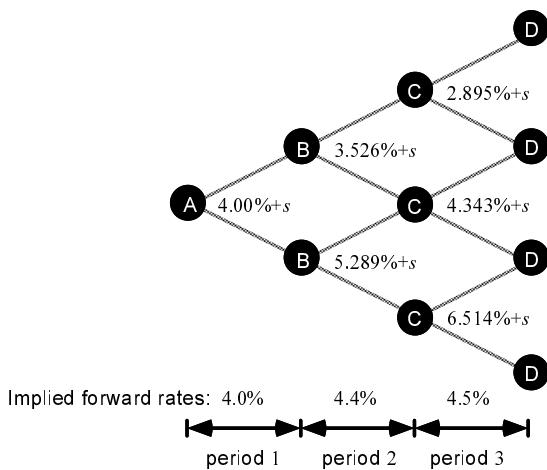


Figure 23.8: SPREAD OVER SHORT RATES OF BINOMIAL INTEREST RATE TREE. This tree is constructed from the calibrated binomial interest rate tree in Fig. 23.7b by adding a constant spread s to each short rate in the tree.

We apply the spread concept to option-free bonds first and will return to the treatment of bonds with embedded options in §27.3.4. The techniques are identical save for the possibility of early exercise, precisely the kind of difference between pricing European and American options under the binomial option pricing model.

In general, if we add a constant amount s to every rate in the binomial interest rate tree, the model price will be a monotonically decreasing, convex function of s . Call this function $p(s)$. For a given market price P , we can employ a root-finding algorithm to solve

$p(s) - P = 0$ for s . Since the root-finding algorithm will use the quadratic-time algorithm in Fig. 23.4 with different s 's, convergence rate of the algorithm is critical.

The Newton-Raphson method converges fast if it starts with a good guess to the root. However, evaluating $p'(s)$ directly by expansion looks intimidating. Fortunately, the tree, already a compact representation of $p(s)$, can be used to evaluate both $p(s)$ and $p'(s)$ with backward induction. Here is the idea. Consider an arbitrary node A in the tree. In the process of computing the model price $p(s)$, a price $p_A(s)$ is computed at A. Node A is associated with a short rate r . Hence, prices computed at A's two successor nodes, B and C, will be discounted by $r + s$ to obtain

$$p_A(s) = c + \frac{p_B(s) + p_C(s)}{2(1 + r + s)},$$

where c denotes the cash flow at A. To compute $p'_A(s)$ as well, node A calculates

$$p'_A(s) = \frac{p'_B(s) + p'_C(s)}{2(1 + r + s)} - \frac{p_B(s) + p_C(s)}{2(1 + r + s)^2}, \quad (23.9)$$

Now, computing $p'_A(s)$ is easy as long as $p'_B(s)$ and $p'_C(s)$ are supplied by nodes B and C. Applying the above procedure inductively will eventually lead to $p(s)$ and $p'(s)$ at the root. See Fig. 23.11 for illustration. This technique, due to Lyuu, is called the **differential tree method** and has many applications [550]. The differential tree method is related to **automatic differentiation** [605].

The differential tree approach appears in Fig. 23.12. Given a spread, Step 1 computes the present value, and Step 2 computes the derivative of the present value according to (23.9). Step 3 is the Newton-Raphson method for the next approximation. The running time depends on the convergence rate of the Newton-Raphson method. If \mathcal{C} represents the number of times the tree is traversed, which takes $O(n^2)$ time, the total running time becomes $O(\mathcal{C}n^2)$. In practice, \mathcal{C} is a small constant. The memory requirement is $O(n)$.

Let us go through a numerical example. Consider a three-year, 5% bond with a market price of 100.569. For convenience, assume the bond pays annual interest. The spread can be calculated to be 50 basis points over the tree. This is verified in Fig. 23.13. In comparison, let's compute the yield spread and static spread of the non-benchmark bond over an otherwise identical benchmark bond. Recall that the static spread is the incremental return over the spot rate curve, whereas the spread based on the binomial interest rate tree is one over the future short rates. Obviously, the spread of a benchmark security is zero.

The yield to maturity of the non-benchmark bond can be calculated to be 4.792%. Now, from the sample term structure, the three-year Treasury has a market price of

$$\frac{5}{1.04} + \frac{5}{(1.042)^2} + \frac{105}{(1.043)^3} = 101.954 \quad (23.10)$$

and a yield to maturity of 4.292%. The yield spread is thus $4.792\% - 4.292\% = 0.5\%$. The static spread can also be found to be 0.5%. So all three spreads turn out to be 0.5% up to round-off errors.

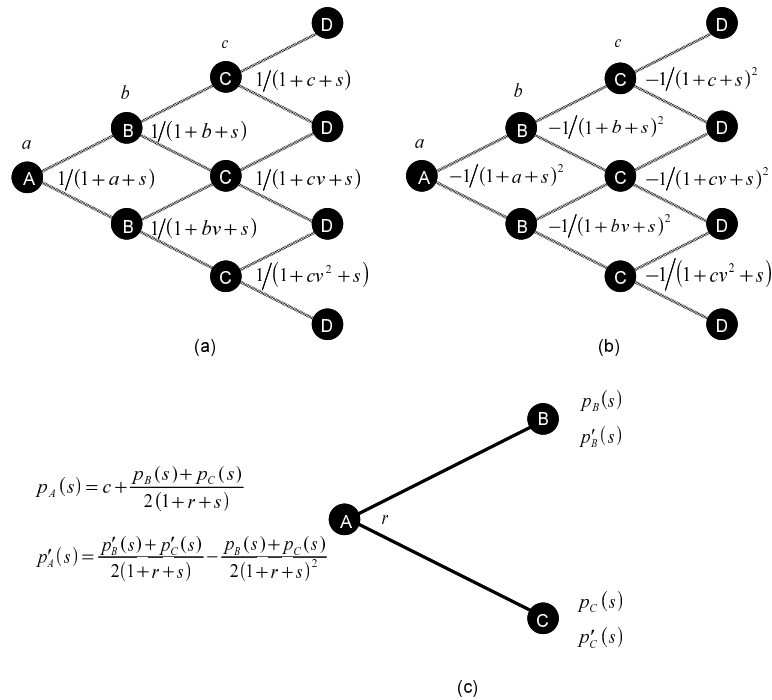


Figure 23.9: THE DIFFERENTIAL TREE METHOD. (a) The original binomial interest rate tree with short rates replaced by the discount factors. (b) The derivatives of the numbers on the tree. (c) The simultaneous evaluation of a function and its derivative with the binomial tree structure using the numbers from (a) and (b).

23.3.2 Interest rate futures

Futures price is a martingale under the risk-neutral probability (see Exercise 13.2.11). So, to compute it, we first use the tree to calculate the underlying security’s prices at the futures contract’s delivery date to which the futures price converges. Then we find the expected values. In Fig. 23.14, for example, we are concerned with a two-year futures contract on a one-year Treasury bill. The futures price is found to be 95.687.

The contract specification for a futures contract may not call for a quote that equals the result of our computation—95.687 in our case. If so, necessary steps have to be taken to convert the theoretical value into one consistent with the specification. The theoretical value, for instance, corresponds to the invoice price of the Treasury bill futures traded on the CBT, but it is the index price that is being quoted.

Programming assignment 23.3.1 Write a program to price Treasury bill futures.

23.3.3 Fixed-income options

Determining the values of fixed-income options with a binomial interest rate tree follows the same logic as the binomial tree algorithm for stock options in Chapter 9. Hence, only numerical examples will be attempted here.

Consider a two-year 99 European call on the three-year, 5% Treasury, assuming the Treasury pays annual interest. From Fig. 23.15, the three-year Treasury’s price minus the

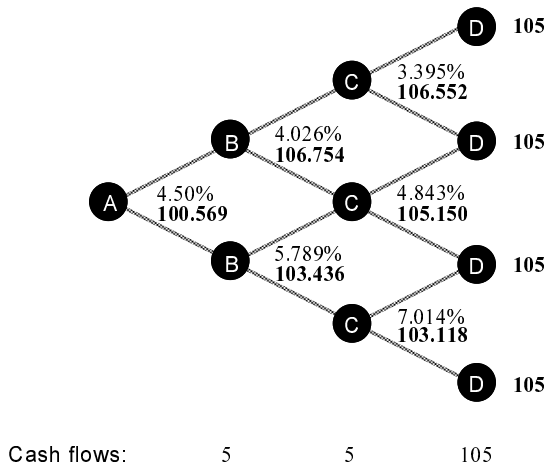


Figure 23.10: THE PRICE TREE WITH SPREAD. Based on the tree in Fig. 23.10, the price tree is computed for a three-year bond paying 5% annual interest. Each node of the tree signifies, besides the short rate, the discounted value of its future cash flows plus the cash flow at that node, if any. The model price is 100.569.

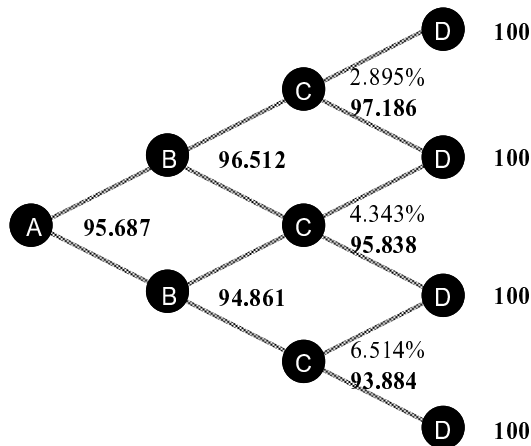


Figure 23.11: INTEREST RATE FUTURES. The price tree is computed for a two-year futures contract on a one-year Treasury bill. C nodes store, besides the short rate, the discounted values of the one-year Treasury bill under the model. A and B nodes calculate the expected values. The computed futures price is 95.687.

\$5 interest could be \$102.046, \$100.630, or \$98.579 two years from now. Since these prices do not include the accrued interest, we should compare the strike price against them. The call is therefore in the money in the first two scenarios, with values of \$3.046 and \$1.630, and out of the money in the last scenario. The option value is calculated to be \$1.458 in Fig. 23.15a.

European interest rate puts can be valued similarly. Consider a two-year 99 European put on the same security. At expiration, the put is in the money only if the Treasury is worth \$98.579 after subtracting the accrued interest. The option value is computed to be \$0.096 in Fig. 23.15b.

If the option is American and the underlying bond generates payments before the option's expiration date, early exercise needs to be considered. The criterion is to compare the intrinsic value against the option value at each node. We leave the details to the reader.

Does the put-call parity still hold? The present value of the strike price is $PV(X) = 99 \times 0.92101 = 91.18$. The Treasury is worth $B = 101.955$. The present value of the interest payments during the life of the options is

$$PV(I) = 5 \times 0.96154 + 5 \times 0.92101 = 9.41275.$$

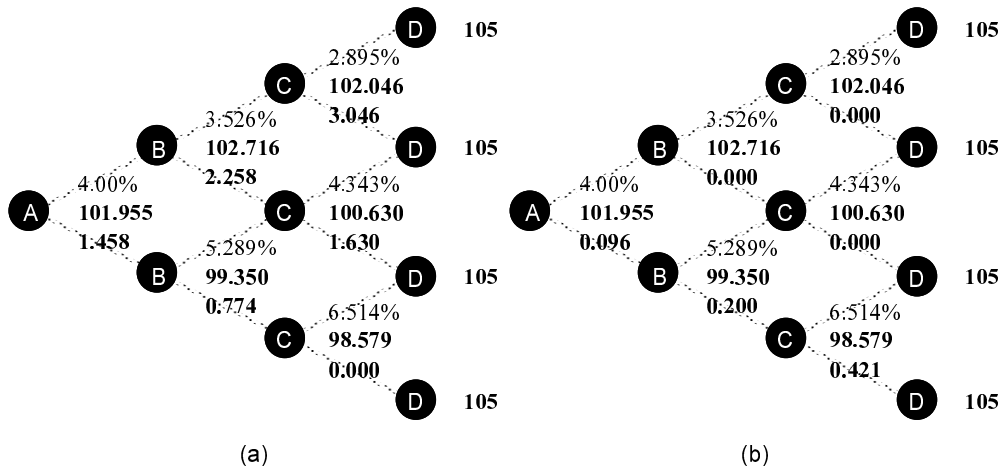


Figure 23.12: EUROPEAN OPTIONS ON TREASURIES. The above price trees are computed for the two-year 99 European (a) call and (b) put on the three-year, 5% Treasury. Each node of the tree signifies the short rate, the Treasury price without the \$5 interest (except the terminal nodes), and the option value. The current price \$101.955 is slightly off compared with (23.10) due to round-off errors.

The call and the put are worth $C = 1.458$ and $P = 0.096$, respectively. Hence,

$$C = P + B - PV(I) - PV(X).$$

The put-call parity is preserved.

23.3.4 Dynamic immunization

For bonds without embedded options, duration can be defined under the binomial interest rate tree as $\sum_i t_i \omega_{t_i}$, where ω_t is the present value of the future cash flow at time t divided by the present value of all future cash flows. This definition, of course, applies to any model. There is evidence that adding the convexity constraint beyond duration matching does not improve performance [328].

23.3.5 Delta (hedge ratio)

One is often interested in knowing how much the option price changes in response to changes in the price of the underlying bond. We measure this relation by **delta (hedge ratio)**, defined as

$$\frac{O_u - O_d}{P_u - P_d}.$$

In the above equation, P_u and P_d denote the bond prices if the short rate moves up and down, respectively. Similarly, O_u and O_d denote the option values if the short rate moves up and down, respectively. Since delta measures the sensitivity of the option value to changes in the underlying bond price, it shows how to hedge one with the other [77]. Take the call and put in Fig. 23.15 as examples. Their deltas are

$$\frac{0.774 - 2.258}{99.350 - 102.716} = 0.441 \quad \text{and} \quad \frac{0.200 - 0.000}{99.350 - 102.716} = -0.059,$$

respectively.

23.3.6 Holding period return analysis

Short rate	Horizon price	Probability
2.895%	0.971865	0.25
4.343%	0.958378	0.50
6.514%	0.938844	0.25

Figure 23.13: HOLDING PERIOD RETURN ANALYSIS. The horizon is two periods.

Analyzing the holding period return with the binomial interest rate tree is straightforward. As an example, for a two-period horizon and based on the zero-coupon bond price dynamics in Fig. 23.8, we obtain the holding period return analysis in Fig. 23.16. If the bond were coupon-bearing, the interim cash flows should be reinvested at the prevailing short rate and added to the horizon price. This component of the horizon price can be derived by forward induction. Note that the probability distribution of the scenario analysis is provided by the model, not exogenously. This is the same as the VaR methodology.

23.4 Volatility Term Structures

The binomial interest rate tree can be used to calculate the yield volatility of zero-coupon bonds. Consider an n -period zero-coupon bond. Find its yield to maturity y_h (y_l , respectively) at the end of the initial period if the rate rises (declines, respectively). The yield volatility for our model is then defined as

$$\frac{1}{2} \ln \left(\frac{y_h}{y_l} \right).$$

Based on the tree in Fig. 23.7b, the two-year zero's yield at the end of the first period is 5.289% if the rate rises and 3.526% if the rate declines. Its yield volatility is then

$$\frac{1}{2} \ln \left(\frac{0.05289}{0.03526} \right) = 20.273\%.$$

Now, consider the three-year zero-coupon bond. If the rate rises, the price of the zero one year from now will be

$$\frac{1}{2} \times \frac{1}{1.05289} \times \left(\frac{1}{1.04343} + \frac{1}{1.06514} \right) = 0.90096.$$

Thus its yield is $\sqrt{\frac{1}{0.90096}} - 1 = 0.053531$. (This is how the term structure dynamics on Page 361 was derived.) If the rate declines, the price of the zero one year from now will be

$$\frac{1}{2} \times \frac{1}{1.03526} \times \left(\frac{1}{1.02895} + \frac{1}{1.04343} \right) = 0.93225.$$

Thus its yield is $\sqrt{\frac{1}{0.93225}} - 1 = 0.0357$. The yield volatility is hence

$$\frac{1}{2} \ln \left(\frac{0.053531}{0.0357} \right) = 20.256\%,$$

slightly less than the one-year yield volatility. Incidentally, this is consistent with the reality that longer-term bonds typically have lower yield volatility than shorter-term bonds. This procedure can be repeated for longer-term zeros to obtain their yield volatilities.

We started with v_i and then derived the volatility term structure. In practice, the steps are reversed. The volatility term structure is supplied by the user along with the term structure of interest rates. The v_i 's—hence the short rate volatilities as well via (23.3)—and the r_i 's are then simultaneously determined. The result is the Black-Derman-Toy model [78].

The binomial interest rate tree and most other term structure models allow the volatility term structure to evolve with time. The volatility term structure supplied by the user is *not* maintained through time. For instance, the user supplies the volatility term structure which results in (v_1, v_2, v_3, \dots) for the tree initially. According to the model, the volatility term structure one period from now will be determined by (v_2, v_3, v_4, \dots) regardless of the rate movement in the first period. This could be contrary to what the user has in mind, which may be (v_1, v_2, v_3, \dots) [147]. This issue will be reexamined in Chapter 26.

Programming assignment 23.4.1 Modify the program of Programming assignment 23.2.7 to output the annualized term structure of yield volatilities as well.